A Theoretical Study of the Photodetachment and Intramolecular Hydrogen-Bonding Energies of Hydrogen Maleate Anions

Shan Xi Tian* and Hai-Bei Li

Hefei National Laboratory for Physical Sciences at Microscale and Department of Chemical Physics, University of Science and Technology of China, Hefei, Anhui 230026, People's Republic of China

Received: January 28, 2007; In Final Form: March 12, 2007

Three low-lying conformers of the hydrogen maleate anions (HMAs) regarding *cis*-HMA(HB) having the $O^-\cdots HO$ intramolecular hydrogen bond (HB), *cis*-HMA(nHB) without the HB, and *trans*-HMA are studied by density functional theory (B3LYP) combined with natural bond orbital (NBO) and atoms-in-molecules (AIM) analyses. The photoelectron spectra of *cis*- and *trans*-HMA conformers recorded by Woo et al. (*J. Phys. Chem. A* **2005**, *109*, 10633) are reassigned on the basis of the present electron propagator theory calculations, indicating the significant energy differences between the Dyson orbitals and canonical molecular orbitals due to the electron-correlation and orbital relaxation effects considered in the electron propagator theory. The NBO associated with the natural resonance theory analyses and AIM electron topological study show that the strong $O^-\cdots HO$ in *cis*-HMA(HB) has the remarkable characteristics of three-center four-electron hyperbond, and the bonding strength of ca. 30 kcal/mol is recommended with the reference calculations of the $HO^-\cdots HOH$ complex. The further calculations for the microhydrated *cis*-HMA(HB) clusters indicate that the $O^-\cdots HO$ bonding strength decreases in water solution.

1. Introduction

Recently, short-strong hydrogen bonds (SSHBs) attract considerable interest because of their possible role in biological activities, particularly in the enzymatic processes.[1] A typical SSHB, the homonuclear O···HO, exhibits a short, linear HB with an extremely low barrier for the hydrogen transfer between two oxygen atoms. This SSHB is also noted as the low-barrier HB (LBHB).[2] A lots of studies have been designed to measure or calculate the strength of this strong HB. On the other hand, differing from the intermolecular HB cases in which the strength can be calculated routinely within a supermolecular scheme,[3] it is rather difficult to calculate the intramolecular HB strength directly from the properties of an unit molecule.[4,5] Hydrogen maleate anion (HMA) and diketone enol are good choice both for the experimental[6] and theoretical[4] studies of the intramolecular LBHB, but the reported solutions for the intramolecular HB strength are problematic. As for HMA shown in Figure 1, two cis and one trans species have been proved to be the low-lying conformers.[4,6] There are arguments on the intramolecular $O^-\cdots HO$ HB strength and its nature in *cis*-HMA(HB). The HB strength of 0.5−5.5 kcal/mol depending on the solvent used has been estimated by the solvent equilibration experiments of Schwartz and Drueckhammer.[6b] The hydrogen maleate is 20 kcal/mol more stable than fumarate, according to the calculations of Garcia-Viloca et al. [4a] The intramolecular $O^-\cdots HO$ HB strength in *cis*-HMA(HB) is predicted theoretically to be 14−28 kcal/mol depending on the choices of the reference structures.[4b] In fact, there are several problems in calculating the intramolecular HB strength via comparison with the reference structure. First, the stabilities of the different conformers strongly depend on the intramolecular interactions such as charge-transfer, electrostatic, and steric repulsive interactions among the groups in this molecule. Second, the intramolecular HB strength cannot be simply derived by comparison between a conformer with HB and another conformer without HB, due to the fact that the other intramolecular interactions are also different between these

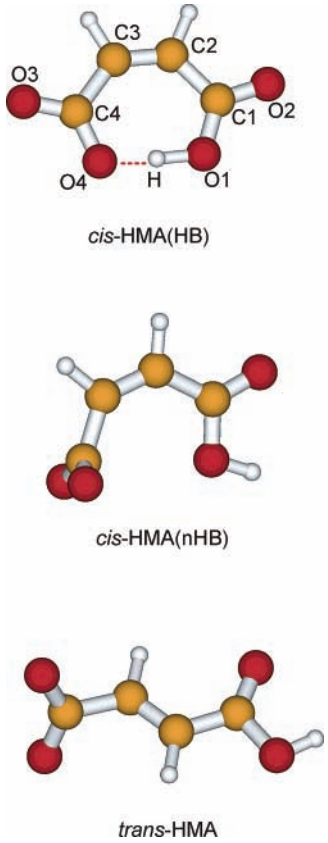

Figure 1. Three low-lying conformers of the hydrogen maleate anions.

* To whom correspondence should be addressed. E-mail: sxtian@ustc.edu.cn.

10.1021/jp070730u CCC: $37.00
Published on Web 04/27/2007

two conformers. At least, one must be circumspective to select the proper reference molecule. Third, although the electrostatic interaction plays role in the normal inter- and intramolecular HBs, the nonelectrostatic contributions, in particular charge-transfer, are also important for the strong intramolecular HB.[4c,5] We have successfully explained that the charge-transfer for the strong intramolecular N···HO HB led to the band splitting in the photoelectron spectrum (PES) of proline.[5a] This method is potentially a solution to estimate the strength of the intramolecular HB.

The anionic intramolecular O$^-$···HO HB is of particular interest because this asymmetrical HB interaction is suspected to form the symmetrical delocalized three-center four-electron (3c−4e) [O···H···O]$^-$ hyperbond in the valence bond (VB) theory.[4d,e] To elucidate the nature of the remarkably strong intramolecular O$^-$···HO HB, an experimental photodetachment study of HMA conformers was performed by Woo et al.[7] Their powerful techniques can distinguish certain conformer produced from the corresponding species via the electrospray ionization through the recording of the PES by photodetachment.[7] There were the distinctly different features between *trans*-HMA and *cis*-HMA PES, and the *cis*-HMA(HB) was assigned to the PES on the basis of the adiabatic detachment energy calculations.[7] However, the higher states were not assigned in the PES, due to the seriously overlapped bands.[7] Moreover, the estimation of the intramolecular O$^-$···HO HB strength 21.5 ± 2.0 kcal/mol by conformational comparison[7] is improper. In this work, we employ the electron propagator theory[8] to predict the photodetachment states for the valence canonical molecular orbitals (MOs) of three low-lying HMA conformers, and make reassignments to the PES. Natural bond orbital (NBO)[9] and atoms-in-molecules (AIM)[10] theorems are utilized to provide insights into the nature of the intramolecular O$^-$···HO HB in *cis*-HMA(HB).

2. Theoretical Methods

Ab initio MO calculations were performed with Gaussian 98 suite of program.[11] The Becke three-parameter hybrid functional combined with Lee−Yang−Parr (LYP) correlation functional (B3LYP)[12] was employed together with 6-311++G(2d,2p) basis set in the calculations. Geometrical parameters of three low-lying HMA conformers, *cis*-HMA(HB) (C_s-symmetry), *cis*-HMA(nHB) (C_s-symmetry), and *trans*-HMA (C_1-symmetry) shown in Figure 1, were fully optimized at the B3LYP/6-311++G(2d,2p) level. The conformations were proved to correspond to the minima on the potential energy surface by the vibrational frequency calculations. The vertical ionization potentials (IP_vs) and electronic property analyses were performed over the optimized geometries.

In contrast to Koopmans' theorem (KT), the energies (ϵ_p) of electron detachment (i.e., IP_v values) correspond to Dyson orbitals,

$$\phi_p(x_1) = \sqrt{N}\int \Psi_N(x_1,x_2,x_3,\cdots,x_N)\Psi^*_{N-1,p}(x_2,x_3,x_4,\cdots,x_N)dx_2dx_3dx_4\cdots dx_N \quad (1)$$

where x_i is the space-spin coordinate of electron i. In the electron propagator formalism,[8] ϵ_p can be calculated in a way similar to the self-consistent procedure

$$[F + \sum(\epsilon_p)]\phi_p = \epsilon_p\phi_p \quad (2)$$

where F is the Fock operator. To overcome the difficulties that the KT frequently predicts the unsatisfied lower IP_v (with 1∼2 eV errors), the partial third-order (P3) approximation considering self-energy effect has been introduced.[13] Then the Dyson orbital can be

$$\phi_p = \sqrt{P}\,\phi_p^{HF} \quad (3)$$

Here P is the pole-strength and the off-diagonal elements of the self-energy matrix are omitted.[13] ϕ_p^{HF} is the canonical (Hartree−Fock) MO wavefucntion. In general, the P3 corrections to the KT results are essential in assignments to PES because all orbital relaxation effects between initial and final states are included in the self-energy operator. The average absolute error is ca. 0.2 eV for the IP_v of the organic molecules.[8a,8b,13] In this work, the IP_v values were predicted at the P3/6-311G(2d,2p) level, and the pole strengths were found to be larger than 0.88.

To reveal the nature and bonding strength of the intramolecular HB, the NBO and AIM analyses were made using the B3LYP wave functions. The NBO analysis transfers the delocalized molecular orbitals into the localized ones that are closely tied to chemical bond concepts. Filled NBOs describe the hypothetical, strictly localized Lewis structure. The interaction between filled (lone pair electrons) σ and antibonding σ^* orbitals represents the deviation of the molecule from the Lewis structure and can be used as a measurement of charge-transfer due to the HB interactions. Since the occupancies of filled NBOs are highly condensed, the charge-transfer can be further treated by the second-perturbation energies $E(2)$

$$E(2) = -n_\sigma\frac{\langle\sigma|F|\sigma^*\rangle^2}{\epsilon_{\sigma^*}-\epsilon_\sigma} = -n_\sigma\frac{F_{ij}^{\,2}}{\Delta\epsilon} \quad (4)$$

where F_{ij} is the Fock matrix element between the NBO i and j, ϵ_σ and ϵ_{σ^*} are the energies of σ and σ^* NBOs, and n_σ is the population (it is a lone pair in the HB complex).[9] The topological features of the electron density ρ_b and its Laplace transform $\nabla^2\rho_b$ at the bond critical points (BCPs) were also computed with the Bader's AIM theory.[10] The NBO5.0[14] and AIM2000[15] programs were used in the above calculations.

The above NBO and AIM analyses were performed to reveal the characteristics of the intramolecular O$^-$···HO HB. Because of the remarkably differences of HMA conformers shown in Figure 1, neither *cis*-HMA(nHB) or *trans*-HMA was a proper reference to predict the O$^-$···HO HB strength using the method proposed before.[5a] An alternative way was to derive it by the energetic calculations for a candidate system HO$^-$···HOH, which exhibited similar properties compared with the C═O$^-$···H−O moiety in *cis*-HMA(HB) (see the following discussion). Thereby, the energetic calculations were further carried out both at the B3LYP and high-level CCSD(T)[16] levels of theory for the HO$^-$···H_2O complex. The binding energies (ΔE_{bind}) was calculated by the energy differences between the complex and free monomers

$$\Delta E_{bind}(\text{ZPVE or TEC}) = E_{tot}^{complex} - E_{tot}^{OH^-} - E_{tot}^{H_2O} \quad (5)$$

Here the zero-point vibrational energy (ZPVE) or thermal energy correction (TEC) was included. The enthalpy and free energy changes (ΔH and ΔG) were also estimated in the similar way. The HB strength (ΔE_{HB}) was obtained with the energy difference between the complex and the monomers therein

$$\Delta E_{HB}(\text{BSSE}) = E_{tot}^{complex}(\text{complex}) - E_{tot}^{OH^-}(\text{complex}) - E_{tot}^{H_2O}(\text{complex}) \quad (6)$$

TABLE 1: Optimized Geometrical Parameters (Bond Length in Å, Angle in Degree) and the Relative Energies (δE in kcal/mol)

	cis-HMA(HB)	*cis*-HMA(nHB)	*trans*-HMA
R(O1H)	1.094	0.965	0.966
R(C1O1)	1.306	1.355	1.382
R(C1O2)	1.227	1.224	1.217
R(C1C2)	1.502	1.457	1.453
R(C2C3)	1.340	1.347	1.343
R(C3C4)	1.517	1.521	1.517
R(C4O3)	1.238	1.248	1.253
R(C4O4)	1.281	1.248	1.247
R(O4$^-$···H)	1.336		
A(O3C4O4)	126.0	130.8	130.5
δE	0.00[a]	19.47[a]	14.66[a]
	0.0[b]	21.4[b]	17.3[b]

[a] This work, B3LYP/6-311++G(2d,2p) + ZPVE corrections. [b] From ref 7, CCSD/aug-cc-pVTZ + ZPVE (B3LYP/aug-cc-pVTZ).

The basis set superposition error (BSSE)[17] was considered by using the whole basis set in the calculations of the total energies of the monomers. To mimic the O$^-$···HO HB strength of *cis*-HMA(HB) in water solution, the microhydrated clusters *cis*-HMA(HB)−$(H_2O)_n$ (n = 1, 2, 3) were studied and compared with the free *cis*-HMA(HB).

3. Results and Discussion

Ionization Potentials and Assignments to PES. The geometrical parameters optimized at the B3LYP/6-311++G(2d,2p) level are listed in Table 1. One can find they are extremely close to the values obtained with the aug-cc-pVTZ basis set.[7] The stabilities with respect to the global minimum *cis*-HMA(HB) are 19.47 and 14.66 kcal/mol for *cis*-HMA(nHB) and *trans*-HMA, respectively. These relative energies δE are also in good agreement with the previous results.[4b,7] In *cis*-HMA(HB), the intramolecular HB distance R(O4$^-$···H) is predicted to be 1.336 Å with angle A(O4$^-$···HO1) = 177.1°, which are comparable with 1.30 Å and 178.09° (MP2/6-31+G(d,p)[4a]), 1.376 Å (QCISD/6-31+G**[4b]), and 1.330 Å and 176.9° (B3LYP/aug-cc-pVTZ[7]). This intramolecular SSHB was regarded as a 3c−4e hyperbond by Gill et al. [4d] We will give the further proves of its hyperbond characteristics in the next section.

The IP_v values obtained from the P3 calculations, together with the KT values, are presented in Table 2. The corresponding experimental data[7] are also shown in Table 2, but the peaks are reassigned according to the present calculations. To our surprise, there are the significant differences for the photodetachment state sequences predicted between the P3 level and the Koopmans' approximation. The valence electron configurations are $(3a'')^2(23a')^2(24a')^2(25a')^2(4a'')^2(5a'')^2$ for *cis*-HMA(HB), $(6a'')^2(22a')^2(7a'')^2(8a'')^2$ for *cis*-HMA(nHB), and $(27a)^2(28a)^2(29a)^2(30a)^2$ for *trans*-HMA. However, their corresponding Dyson orbital sequences are altered remarkably. In the canonical MO energy-level sequences (i.e., the KT sequences), the Dyson orbitals are plotted in Figures 2 and 3 for *cis*-HMA(HB) and *trans*-HMA, respectively. Although it is well-known that the P3 results often produce the different ordering of cationic states with respect to the KT,[8a,8b,13] such differences observed in this work are really profound. This order variance is mostly due to the electron correlation and orbital relaxation included in the P3 method.[13]

In the PES of *cis*-HMA, there is a huge shoulder in the low-energy range 4.9−6.0 eV.[7] The absence of *cis*-HMA(nHB) was proved by the adiabatic IP values calculated at the higher level of theory, namely, 4.26 eV for *cis*-HMA(nHB) and 4.85 eV for *cis*-HMA(HB).[7] The large IP_v difference 1.11 eV (5.30−4.19 eV for the lowest IP_v values) obtained by the P3 method supports this conclusion. Although the band at $IP_v \sim 5.7-6.0$ eV for the higher states cannot be resolved from the spectrum,[7] a plateau around 6.0 eV implies that there may be one or more cationic states. In fact, the P3 calculations predict B^2A'' (5.89 eV, ionization from 4a″) and C^2A'' states (6.01 eV, ionization from 3a″). Another state A^2A' is predicted at 5.60 eV, and correspondingly a shoulder around 5.5 eV can be observed in the PES. D^2A'' state at 6.32 eV is comfortably close to the experimental IP_v 6.31 eV. The sharp peak assigned improperly with C state[7] may be due to the serious overlap between C^2A''

TABLE 2: Vertical Detachment Energies (VDEs in eV) Predicted at the P3/6-311G(2d,2p) Level and Within Koopmans' Theorem (KT) in Comparison with the Experimental Data

	VDE_{theor}		
assignment[a]	P3	KT	VDE_{exptl}[b]
	cis-HMA(HB), C_s-symmetric		
X^2A'	5.30	7.17(25a′)	(5.19)[c]
A^2A'	5.60	7.23(24a′)	
B^2A''	5.89	7.00(4a″)	
C^2A''	6.01	7.83(3a″)	
D^2A''	6.32	6.70(5a″)	6.31
	cis-HMA(nHB),C_s-symmetric		
X^2A'	4.19	5.76(22a′)	
A^2A''	4.32	5.46(8a″)	
B^2A''	4.33	5.55(7a″)	
C^2A''	6.30	7.08(6a″)	
	trans-HMA, C_1-symmetric		
X^2A	4.36	5.95(28a)	4.22
A^2A	4.44	5.53(30a)	(4.51)
B^2A	4.47	5.70(29a)	4.51
C^2A	6.23	7.05(27a)	6.23

[a] According to the present P3 results. [b] From ref 7. [c] Calculated at the CCSD/aug-cc-pVTZ level in ref 7.

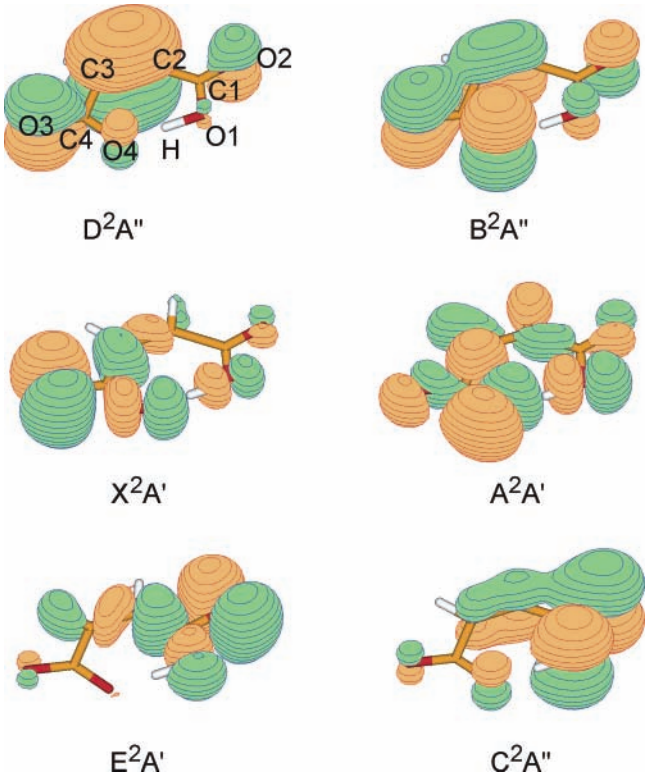

Figure 2. Dyson orbitals of *cis*-HMA(HB). The maps are presented from the upper-left to below-right in energy level sequence of the canonical molecular orbitals, with contour plots = ±0.03.

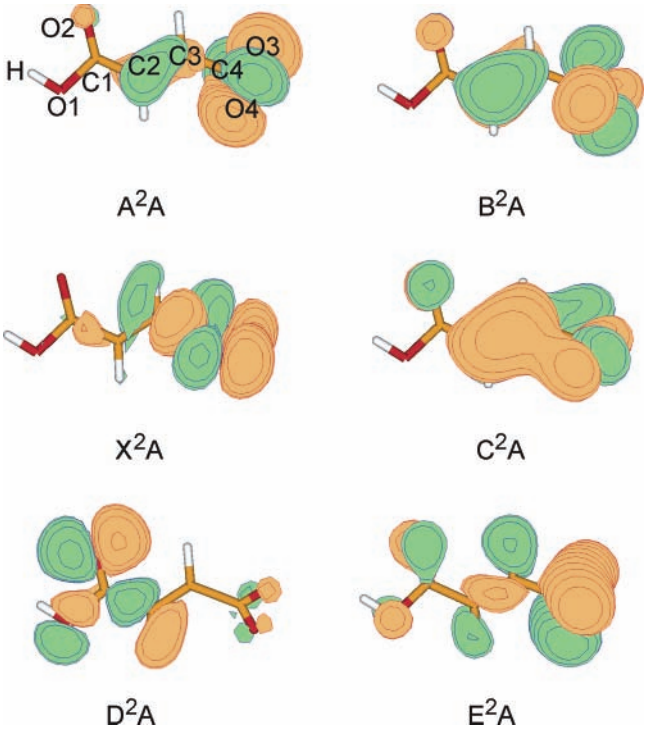

Figure 3. Dyson orbitals of *trans*-HMA. The maps are presented from the upper-left to below-right in energy level sequence of the canonical molecular orbitals, with contour plots = ±0.03.

and D^2A'' states predicted by the P3 calculations. Moreover, as shown in Figure 2, these two states can lead to the photodetachment-excited vibrations for the C2═C3 π orbital, which has been observed in the spectrum.[7]

Four cationic states, X, A (at 4.22 eV), B (at 4.51 eV), and C (at 6.23 eV), were assigned in the PES of *trans*-HMA.[7] They are reassigned precisely according to the present P3 calculations. Namely, they are X^2A (4.36 eV), A^2A (4.44 eV), B^2A (4.47 eV), and C^2A (6.23 eV), corresponding to the ionizations from the canonical MOs 28a, 30a, 29a, and 27a. Because of the vibrational structures in a range 4.2∼ 5.0 eV, the previous assignments to the PES with A and B states[7] are improper, while three states (X, A, and B) should be assigned. In Figure 3, the Dyson orbitals (A^2A and B^2A) show the predominant electron distributions of C4O3O4 group. This indicates the ionizations should yield the OCO vibrations, as the interpretation given by Woo et al.[7] The present P3 predictions are generally in good agreement the experimental data.

Hydrogen-Bonding Strength and Electronic Properties of O⁻···HO in *cis*-HMA(HB). The linear O⁻···HO and the other homonuclear HBs have been investigated both by experiments[6] and theoretical calculations.[4,7] It is interesting that the intramolecular O⁻···HO in *cis*-HMA(HB) was found to depend on the solution polarity. This LBHB becomes a symmetric [O···H···O]⁻ HB in a nonploar solvent.[4a] Moreover, the cis conformer was greatly preferred in aprotic solvents while the trans conformer was found in protic solvents.[6b] The previous theoretical approaches provide the energetics of the height of the low barrier for the hydrogen transfer,[4a,b,d,e] and the electron topological analyses have been made for insights into the nature of electronic structures.[4a−c] However, it is still a challenge to estimate the intrmolecular HB strength. Three typical methods, the conformational analysis,[18] and isodesmic reaction,[19] and the ortho−para comparison[20] methods have been proposed. As for the strong intramolecular O⁻···HO in *cis*-HMA(HB), the strength has been estimated to be 14−28 kcal/mol by the conventional

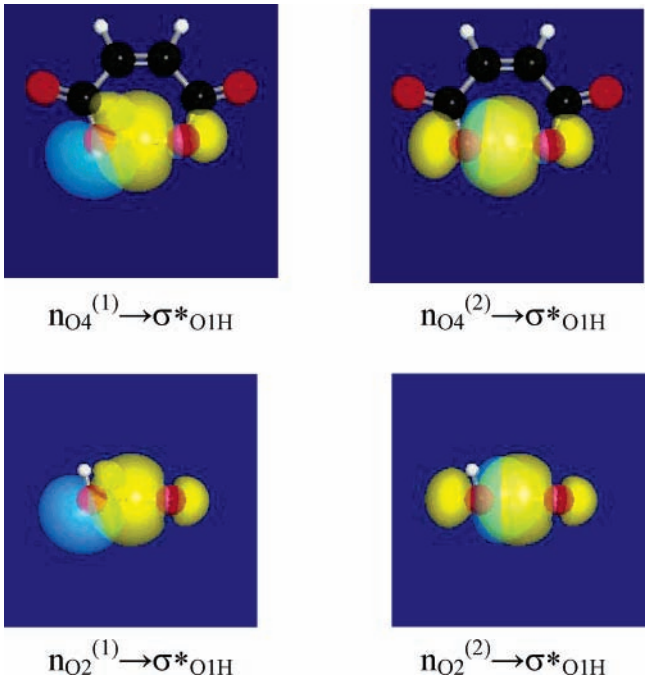

Figure 4. Charge-transfer interactions in *cis*-HMA(HB) (the upper panels) and HO⁻···HOH (the below panels) based on the NBO analyses. $n_O^{(1)}$ and $n_O^{(2)}$ denote the lone-pair orbitals of O atom in the different directions respective to OH bond, and σ^*_{OH} is the antibond.

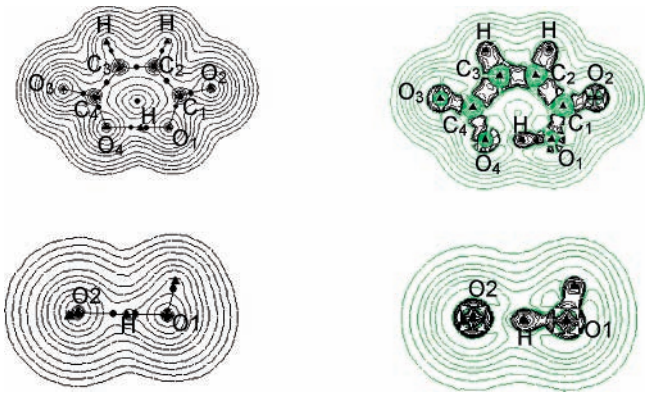

Figure 5. Contour maps of electron density ρ (the left) and the Laplacian $\nabla^2\rho$ (the right) of *cis*-HMA(HB) and HO⁻···HOH. The molecular graphs (solid triangles) are superimposed. Lines connecting the nuclei are the bond paths and the small dots along them represent the bond critical points. Green lines denote regions of electronic charge connection, and black lines denote regions of electronic charge depletion. The contours of the $\nabla^2\rho$ increase (+)/decrease (−), respectively, from the zero contour in the order $\pm 2 \times 10^{-n}$, $\pm 4 \times 10^{-n,}$ $\pm 8 \times 10^{-n,}$ with n beginning from 3 and decreasing in steps of unity. The same set of contours is used through all figures.

conformational analyses.[4,7] The problem of this method is that only the normal electrostatic interaction is stressed, while an additional covalent interaction energy should be considered[4c] for the LBHBs and SSHBs with the polar covalent bonding characteristics.[6b] A proper reference system, HO⁻···HOH, is selected to estimate the intramolecular HB strength of *cis*-HMA(HB), because these two HB moieties are extremely similar. First, the HB length O⁻···H in HO⁻···H_2O is 1.436 Å predicted at the B3LYP/6-311++G(2d,2p) level, which is close to that in *cis*-HMA(HB). Second, the natural atomic populations of the HB moieties indicate that the negative unit charge is mostly embedded on C4O3O4 group in *cis*-HMA(HB) or O2H radical in the HO⁻···H_2O complex. Third, as shown in Figures 4 and 5 and Tables 3−5, the hyperconjugative interactions, bonding

TABLE 3: Hyperconjugative Interaction Energies of *cis*-HMA(HB) and HO⁻···HOH

	NBO Analysis			
	charge-transfer[a]	$\delta\epsilon$(au)	F_{ij}(au)	E(2) (kcal/mol)
	cis-HMA(HB)			
B3LYP/6-311G(2d,2p)	$n_{O4}^{(1)} \rightarrow \sigma^*_{O1H}$	0.90	0.085	9.35
	$n_{O4}^{(2)} \rightarrow \sigma^*_{O1H}$	0.71	0.241	100.56
B3LYP/6-311++G(2d,2p)	$n_{O4}^{(1)} \rightarrow \sigma^*_{O1H}$	0.92	0.087	9.58
	$n_{O4}^{(2)} \rightarrow \sigma^*_{O1H}$	0.72	0.242	99.85
	HO⁻···HOH			
B3LYP/6-311++G(2d,2p)	$n_{O2}^{(1)} \rightarrow \sigma^*_{O1H}$	0.94	0.071	6.17
	$n_{O2}^{(2)} \rightarrow \sigma^*_{O1H}$	0.72	0.247	105.14

[a] See discussion in text and Figure 4.

TABLE 4: Natural Bond Orders in *cis*-HMA(HB) and HO⁻···HOH

cis-HMA	O1H	O4⁻···H
	B3LYP/6-311G(2d,2p)	
total	0.582	0.314
covalent	0.211	0.068
ionic	0.372	0.246
	B3LYP/6-311++G(2d,2p)	
total	0.575	0.323
covalent	0.206	0.068
ionic	0.368	0.256
HO2⁻···HO1H	O1H	O2⁻···H
	B3LYP/6-311++G(2d,2p)	
total	0.620	0.379
covalent	0.206	0.080
ionic	0.414	0.299

TABLE 6: Energies of the Hydrogen-Bonding Complex HO⁻···HOH Used To Simulate the Intramolecular Hydrogen-Bonding Interaction in *cis*-HMA(HB)[a]

	B3LYP	CCSD(T)
ΔE_{bind}(ZPVE)[a]	28.35	26.94
ΔE_{bind}(TEC)[b]	28.98	27.57
ΔH_{bind}	29.58	28.16
ΔG_{bind}	22.11	20.73
ΔE_{HB}(BSSE)[c]	38.85	30.89

[a] Including the zero-point vibrational energy (ZPVE) correction. [b] Including the thermal energy correction ($T = 298.15$ K). [c] Including the superposition basis set error (BSSE) correction.

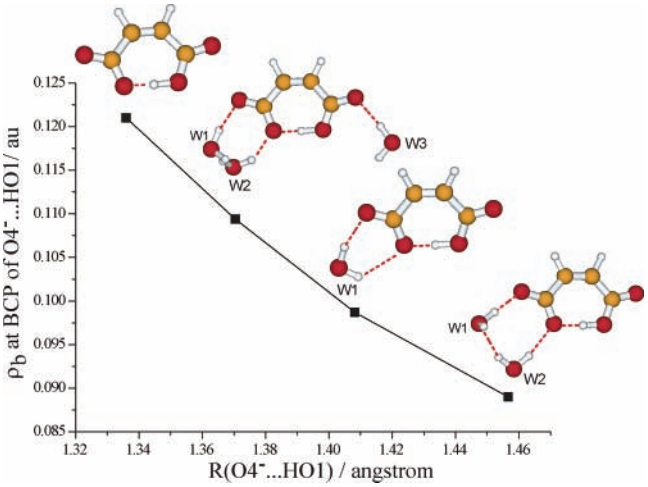

Figure 6. Plot of the electron density ρ_b at BCP in terms of the O4⁻···HO1 hydrogen bond length to simulate the solution effect for *cis*-HMA(HB).

indexes, and electron densities are extremely similar for these two HB moieties. Basically, the strong hyperconjugative interaction energies (99.85 kcal/mol for *cis*-HMA(HB) and 105.14 kcal/mol for HO⁻···H_2O) of $n_O \rightarrow \sigma^*_{OH}$ and the high ρ_b values (0.1210 au for *cis*-HMA(HB) and 0.1176 au for HO⁻···H_2O) at the BCPs indicate these two HBs have comparable strengths. Thereby, it is reasonable to estimate the intramolecular HB strength in *cis*-HMA(HB) using the similar one in HO⁻···H_2O.

ΔE_{bind}(ZPVE), ΔE_{bind}(TEC), ΔH_{bind}, ΔG_{bind}, and ΔE_{HB}(BSSE) values calculated according to eqs 5 and 6 are given in Table 6. ΔE_{HB}(BSSE) values obtained at the B3LYP and CCSD(T) levels of theory are a little larger than the previously reported data. Here we recommend that the HB strength of O⁻···HO in *cis*-HMA(HB) is about 30 kcal/mol. In the proline conformers, the strong intramolecular N···HO HB leads to the high IP_v value of the canonical highest-occupied MO having the predominant lone-pair of N atom.[5a] In that work, the N···HO HB strength can be derived from the IP_v value difference between the conformers with and without the N···HO HB, because those two conformers are extremely similar in structures except for the HBs.[5a] However, it is unfeasible that the O⁻···HO bonding strength in *cis*-HMA(HB) 21.6 kcal/mol was obtained according to the adiabatic IP difference between the trans/cis conformers or 21.4 kcal/mol from the relative stability energy between *cis*-HMA(HB) and *cis*-HMA(nHB).[7] The internal COO^- group rotations in HMA should yield the great changes of the other intramolecular interactions, e.g., steric-repulsive, electrostatic interactions, etc. As for the intramolecular N···HO HB strength in proline,[5a] two similar conformers having the same pyrrolidine puckering ring, i.e., Ia and IIa, or Ib and IIb, are selected; thus, the conformational analysis method is reliable in that case.

To elucidate the solvent effects on this HB strength which has been observed by Schwartz and Drueckhammer,[6b] the microhydrated *cis*-HMA(HB) clusters are studied in this work. In Figure 6, the ρ_b values at the BCPs of O⁻···HO are distinctly different in the various clusters. Moreover, the O⁻···HO HB lengths are sensitive to the hydrated positions around *cis*-HMA(HB). The intermolecular HB interactions between two water molecules (w1 + w2) and the COO^- group result in the significant elongation of O⁻···HO HB length. In general, the

TABLE 5: Topological Properties in (au) of the Electronic Charge Density in the BCPs of *cis*-HMA(HB) and HO⁻···HOH Predicted at the B3LYP/6-311++G(2d,2p) Level[a]

bond	ρ_b	$\nabla^2\rho_b$	λ_1	λ_2	λ_3	G_b	V_b	e	$\lvert\lambda_1\rvert/\lambda_3$	G_b/ρ_b	$\lvert V_b\rvert/G_b$
					cis-HMA(HB)						
O1H	0.2428	−1.2388	−1.0241	−1.0115	0.7968	0.0894	−0.3991	0.0125	1.2853	0.3682	4.4642
O4⁻···H	0.1210	0.0318	−0.3308	−0.3249	0.6875	0.0784	−0.0705	0.0182	0.4812	0.6479	0.8992
					HO2⁻···HO1H						
O1H	0.2204	−0.9406	−0.8669	−0.8481	0.7744	0.0849	−0.3201	−0.2352	1.1194	0.3852	3.7703
O2⁻···H	0.1176	0.0162	−0.3122	−0.3040	0.6324	0.0712	−0.0671	0.0041	0.4937	0.6054	0.9424

[a] See text for the explanation of symbols.

SCHEME 1: Resonance Structure of O4$^-$···HO1 with Weights Predicted with the B3LYP/6-311++G(2d,2p) Wave Functions

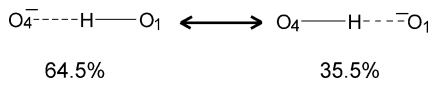

high ρ_b value (0.1210 au) decreases when *cis*-HMA(HB) is combined with more water molecules via intermolecular HBs. According to our previous conclusion that the HB strength is proportional to the ρ_b value,[23] the O$^-$···HO HB strength in water solution decreases with ca. 10−20 kcal/mol.

On the other hand, the intramolecular O$^-$···HO in *cis*-HMA(HB) is regarded as a hyperbond.[4d,e] It is interesting that the VB ionic-resonance picture is truly capable to describe this strong HB. The NBO energy differences $\delta\epsilon$, the NBO wave function overlaps (Fock matrixes) F_{ij}, and the second-order perturbation energies $E(2)$ associated with the predominant charge-transfers $n_{O4} \rightarrow \sigma^*_{O1H}$ are shown in Table 3. Here $n_{O4}^{(1)}$ and $n_{O4}^{(2)}$ denote the lone-pair orbitals of O4 atom in the different directions respective to O1H bond, as shown in Figure 4. It is obvious that the head-to-head $n_{O4}^{(2)}$ orbital is more significantly overlapped with the antibond σ^*_{O1H} than the $n_{O4}^{(1)}$ orbital. Thereby, ca. 100 kcal/mol energy for the former is much larger than the latter. The different basis sets used in the calculations scarcely affect the results. The fundamental feature of this HB and the similar LBHB and SSHB is of electrostatic interaction[4c] as well as charge-transfer. As shown in Scheme 1, the resonance O$^-$···HO ↔ OH···O$^-$ presents some chemical bonding characteristics between O4$^-$ and H atoms. This resonance and the large charge-transfer energy $E(2)$ (ca. 100 kcal/mol) imply that the electron distributions of the canonical MOs 25a′ and 24a′ should be delocalized. Coulson pointed out that the VB ionic-resonance picture is primarily equivalent to the 3c−4e hyperbond.[21] The present natural resonance theory (NRT)[22] analyses show some possibilities (i.e., percentages) in which O1−H is broken while O4−H is formed, and others with the contrary processes. Thereby, the percentages for the respective cases are summarized, then 64.5% and 35.5% weights are predicted for O4$^-$···HO1 and O4H···O1$^-$, respectively, at the B3LYP/6-311++G(2d,2p) level. The bond orders among O4$^-$···HO1 are given in Table 4. The total natural bond order of O1H is much less than unit, while that for O4$^-$···H is a little high. The ionic contribution is predominant, i.e., ca. 0.37 for O1H and ca. 0.25 for O4$^-$···H. All of the above points suggest that the O4$^-$···HO1 should be a 3c−4e hyperbond.

The AIM analyses for the O4$^-$···HO1 HB in *cis*-HMA(HB) are performed using the electron density distributions calculated with the B3LYP/6-311++G(2d,2p) method. In the AIM theorem,[10] the characteristics of electron-shared interactions (i.e., covalent bond) have the large ρ_b values, $\nabla^2\rho_b < 0$, $|\lambda_1|/\lambda_3 > 1$, and $G_b/\rho_b < 1$ at the (3, −1) BCP, where G_b and V_b (in Table 5) are the local kinetic energy density and potential at the BCP. The total energy $E_e = G_b + V_b$, indicating the steric repulsive (here 4.95 kcal/mol for the O4$^-$···H BCP) interaction. Moreover, the Laplacian of ρ_b has the relationship with G_b and V_b,

$$h^2/4m\nabla^2\rho_b = 2G_b + V_b \qquad (7)$$

and

$$\nabla^2\rho_b = \frac{\partial^2\rho_b}{\partial x^2} + \frac{\partial^2\rho_b}{\partial y^2} + \frac{\partial^2\rho_b}{\partial z^2} = \lambda_1 + \lambda_2 + \lambda_3 \qquad (8)$$

On the other hand, the normal HB has such criteria: (i) the existence of a BCP and a ring critical point (RCP); (ii) ρ_b = 0.002−0.04 au; (iii) $\nabla^2\rho_b > 0$, and in a range of 0.02−0.15 au.[24] In Figure 5, the electron density map (the upper) shows there are a BCP along the O4$^-$···HO1 bond and a RCP (circle points) at the middle of the seven-atom ring O4HO1C1C2C3C4. The ρ_b and $\nabla^2\rho_b$ at the O4$^-$···H BCP fall in the scope of the HB values, but the ρ_b values are much larger than the normal values. In comparison with the related values at the BCP of O1H, the BCP of O4$^-$···H has the similar G_b and the ellipticity ϵ values, but the much smaller ρ_b and $|\lambda_1|/\lambda_3$ (less than 1). This indicates that the O4$^-$···H may be the abnormal HB. Moreover, the much smaller ρ_b at the O1H BCP[25] is due to the strong interactions between O1H and O4$^-$. In the $\nabla^2\rho_b$ contour map of *cis*-HMA(HB) in Figure 5, the concentration ($\nabla^2\rho_b > 0$) and depletion ($\nabla^2\rho_b < 0$) of the electron charge density are plotted with the green and black lines, respectively. They show a weak O1H covalent bond and an ionic bond O4$^-$···H. This is in line with the NBO conclusion that O4$^-$···HO1 is an ionic 3c−4e hyperbond. The similarity between the HO$^-$···HOH and O4$^-$···HO1 in *cis*-HMA(HB) implies that the intermolecular O$^-$···HO HB in the former complex should also exhibit the hyperbond characteristics.

4. Conclusion

Three low-lying conformers of HMAs, *cis*-HMA(HB) having the O$^-$···HO intramolecular HB, *cis*-HMA(nHB) without the HB, and *trans*-HMA, are studied by ab initio calculations combined with the NBO and AIM analyses. The electron propagator theory with the P3 approximation is used to predict the IP_v values for assignments to the PES recorded by Woo et al.[7] Two important conclusion are addressed: (1) The first state shown in the *cis*-HMA(HB) PES is not corresponding to photodetachment from the highest-occupied MO. The electron-correlation and orbital relaxation effects included in the electron propagator theory lead to the significant energy sequence alternations between the Dyson orbitals and canonical MOs. The reassignments have been made on the basis of the present theoretical IP_v values. (2) To elucidate the nature of O$^-$···HO HB in *cis*-HMA(HB), the NBO associated with the NRT and AIM electron topological analyses are performed. This strong intramolecular HB has the remarkable characteristics of the ionic 3c−4e hyperbond, and the strength ca. 30 kcal/mol is recommended from the energetic calculations for the HO$^-$···HOH complex. Although the intermolecular HB O$^-$···H in this complex exhibits similar characteristics with respect to that in *cis*-HMA(HB), the small differences can also be found. A more direct strategy, i.e., the intramolecular HB strength derived without any reference systems, is being developed in our group. The solution effect on this HB strength is also investigated by the calculations for the microhydrated *cis*-HMA(HB) clusters, indicating the strength decreases because of the existence of intermolecular HBs between water and *cis*-HMA(HB).

Acknowledgment. This work is supported by the National Natural Science Foundation of China (NNSFC Grant No. 20503026 and 20673105). The reviewers of this manuscript are acknowledged for their valuable comments.

References and Notes

(1) (a) Gerlt, J. A.; Kozarich, J. W.; Keynon, G. L.; Gassman, P. G. *J. Am. Chem. Soc.* **1991**, *113*, 9667. (b) Cleland, W. W.; Kreevoy, M. M. *Science* **1994**, *264*, 1887. (c) Gerlt, J. A.; Gassman, P. G. *Biochemistry* **1993**, *32*, 11943.

(2) (a) Frey, P. A.; Whitt, S. A.; Tobin, J. B. *Science* **1994**, *264*, 1972. (b) Cleland, W. W.; Kreevoy, M. M. *Science* **1995**, *269*, 104. (c) Frey, P. A. *Science* **1995**, *269*, 104. (d) Lin, J.; Frey, P. A. *J. Am. Chem. Soc.* **2000**, *122*, 11258.

(3) (a) Scheiner, S. *Hydrogen Bonding*; Oxford University Press: New York, 1997. (b) Steiner, T. *Angew. Chem., Int. Ed. Engl.* **2002**, *41*, 48. (c) Hobza, P.; Havlas, Z. *Chem. Rev.* **2000**, *100*, 4253.

(4) (a) Garcia-Viloca, M.; Gonzalez-Lafont, A.; Lluch, J. M. *J. Am. Chem. Soc.* **1997**, *119*, 1081. (b) Bach, R. D.; Dmitrenko, O.; Glukhovstev, M. N. *J. Am. Chem. Soc.* **2001**, *123*, 7134. (c) Schiøtt, B.; Iversen, B.; Madsen, G. K. H.; Larsen, F. K.; Bruice, A. T. *Proc. Natl. Acad. Sci. U.S.A. (PNAS)* **1998**, *95*, 12799. (d) Gilli, P.; Bertolasi, V.; Ferretti, V.; Gilli, G. *J. Am. Chem. Soc.* **1994**, *116*, 909. (e) Gilli, P.; Bertolasi, V.; Ferretti, V.; Gilli, G. *J. Am. Chem. Soc.* **2004**, *126*, 3845. (f) McAllister, M. A. *Can. J. Chem.* **1997**, *75*, 1195.

(5) (a) Tian, S. X.; Yang, J. *Angew. Chem., Int. Ed.* **2006**, *45*, 2069. (b) Tian, S. X. *J. Phys. Chem. A.* **2006**, *110*, 3961. (c) Tian, S. X. *J. Chem. Phys.* **2005**, *123*, 24310.

(6) (a) Perrin, C. L.; Thoburn, J. D. *J. Am. Chem. Soc.* **1992**, *114*, 8559, and references cited therein. (b) Schwartz, B.; Drueckhammer, D. G. *J. Am. Chem. Soc.* **1995**, *117*, 11902.

(7) Woo, H.-K.; Wang, X.-B.; Wang, L.-S.; Lau, K.-C. *J. Phys. Chem. A* **2005**, *109*, 10633.

(8) (a) Ortiz, J. V.; Zakrzewski, V. G. *J. Chem. Phys.* **1996**, *105*, 2762. (b) Ferreira, A. M.; Seabra, G.; Dolgounitcheva, O.; Zakrzewski, V. G.; Ortiz, J. V. In *Quantum-Mechanical Prediction of Thermochemical Data*; Cioslowski, J. Ed.; Kluwer: Dordrecht, The Netherlands, 2001; p131. (c) Linderberg, J.; Öhrn, Y. *Propagators in Quantum Chemistry*; Academic Press: New York, 1973.

(9) Reed, A.; Curtiss, L. A.; Weinhold, F. *Chem. Rev.* **1988**, *88*, 899.

(10) Bader, R. F. W. *Atoms in Molecules: A Quantum Theory*; Clarendon: Oxford, U.K., 1990.

(11) Frisch, M. J.; Trucks, G. W.; Schlegel, H. B.; Scuseria, G. E.; Robb, M. A.; Cheeseman, J. R.; Zakrzewski, V. G.; Montgomery, J. A., Jr.; Stratmann, R. E.; Burant, J. C.; Dapprich, S.; Millam, J. M.; Daniels, A. D.; Kudin, K. N.; Strain, M. C.; Farkas, O.; Tomasi, J.; Barone, V.; Cossi, M.; Cammi, R.; Mennucci, B.; Pomelli, C.; Adamo, C.; Clifford, S.; Ochterski, J.; Petersson, G. A.; Ayala, P. Y.; Cui, Q.; Morokuma, K.; Malick, D. K.; Rabuck, A. D.; Raghavachari, K.; Foresman, J. B.; Cioslowski, J.; Ortiz, J. V.; Baboul, A. G.; Stefanov, B. B.; Liu, G.; Liashenko, A.; Piskorz, P.; Komaromi, I.; Gomperts, R.; Martin, R. L.; Fox, D. J.; Keith, T.; Al-Laham, M. A.; Peng, C. Y.; Nanayakkara, A.; Gonzalez, C.; Challacombe, M.; Gill, P. M. W.; Johnson, B.; Chen, W.; Wong, M. W.; Andres, J. L.; Gonzalez, C.; Head-Gordon, M.; Replogle, E. S.; Pople, J. A. *GAUSSIAN 98*; Gaussian, Inc.: Pittsburgh, PA, 1998.

(12) (a) Becke, A. D. *J. Chem. Phys.* **1993**, *98*, 5648. (b) Lee, C.; Yang, W.; Parr, R. G. *Phys. Rev. B.* **1988**, *41*, 785.

(13) Ortiz, J. V. *J. Chem. Phys.* **1996**, *104*, 7599.

(14) Glendening, E. D.; Badenhoop, J. K.; Reed, A. E.; Carpenter, J. E.; Bohmann, J. A.; Morales, C. M.; Weinhold, F. *NBO 5.0*; Theoretical Chemistry Institute: University of Wisconsin, Madison, WI, 2001.

(15) *AIM 2000*: A Program to Analyze and Visualize Atoms in Molecules; http://www.aim2000.de/.

(16) (a) Pople, J. A.; Krishnan, R.; Schlegel, H. B.; Binkley, J. S. *Int. J. Quantum Chem.* **1978**, *15*, 545. (b) Scuseria, G. E.; Schaefer, H. F. III *J. Chem. Phys.* **1989**, *90*, 3700.

(17) Boys, S. F.; Bernardi, F. *Mol. Phys.* **1970**, *19*, 553.

(18) (a) Kovacs, A.; Szabo, A.; Hargittai, I. *Acc. Chem. Res.* **2002**, *35*, 887. (b) Zhang, H.-Y.; Sun, Y.-M.; Wang, X.-L. *Chem.—Eur. J.* **2003**, *9*, 502.

(19) (a) Rozas, I.; Alkorta, I.; Elguero, J. *J. Phys. Chem. A* **2001**, *105*, 10462. (b) Pratt, D. A.; de Heer, M. I.; Mulder, P.; Ingold, K. U. *J. Am. Chem. Soc.* **2001**, *123*, 5518.

(20) Estacio, S. G.; do Couto, P. C.; Cabral, B. J. C.; da Piedade, M. E. M.; Simoes, J. A. M. *J. Phys. Chem. A* **2004**, *108*, 10834.

(21) Coulson, C. A. *J. Chem. Soc.* **1964**, 1442.

(22) (a) Glendening, E. D.; Weinhold, F. *J. Comput. Chem.* **1998**, *19*, 593. (b) Glendening, E. D.; Weinhold, F. *J. Comput. Chem.* **1998**, *19*, 610. (c) Glendening, E. D.; Badenhoop, J. K.; Weinhold, F. *J. Comput. Chem.* **1998**, *19*, 628.

(23) Tian, S. X. *J. Phys. Chem. B.* **2004**, *108*, 20388.

(24) Koch, U.; Popelier, P. L. A. *J. Phys. Chem.* **1995**, *99*, 9747.

(25) As for the OH bond in methanol, $\rho_b = 0.3778$ au, $\nabla^2\rho_b = -2.7066$ au, $|\lambda_1|/\lambda_3 = 1.9838$, and $|\lambda_1|/\lambda_3 > 1$, $G_b/\rho_b = 0.2149$ au at the BCP are obtained by the B3LYP/6−311+G(2d,2p) calculations.